Inkjet Printers Linearization Using 3D Gradation Curves

Oleg B. Milder[1], Dmitry A. Tarasov[1,2], Marina Yu. Titova[1]

[1]Ural Federal University, IRIT, Mira, 32, Ekaterinburg 620002 RUSSIA;
and [2]Institute of Industrial Ecology UB RAS, Kovalevskaya str., 20, Ekaterinburg 620990 RUSSIA
datarasov@yandex.ru

Abstract. A new approach based on 3D gradation curves is suggested as a further development of gradation curves for the inkjet systems linearization. The curves are considered in terms of 3D curves of differential geometry. The 3D curves, as well as their calculating method, are defined and offered as a powerful tool for the inkjet printers linearization and further profile-making. Information that might be derived from the curves is discussed. Preliminary results show broad application opportunity of the proposed method.

Keywords: Gradation trajectories, inkjet, linearization, profile, dotgain

1 Introduction

When setting up the color in inkjet printing systems, the first-stage-problem before the profiling is limitation of the ink supply because further linearization and calibration are strongly dependent on this parameter. Moreover, ink limitation serves to dose the amount of ink that might be sent by RIP to the print head, so as to fix the standard conditions for further profile making. On the other hand, the maximum useful or wanted ink percentage is often less than 100%, thus, reducing the percentage as such becomes the second goal of ink limitation. The need of such a limitation is caused by many factors, primarily, the physics-chemical processes of the inksubstrate interaction, in particular, for non- or weak-absorbent substrates. When several colors are printed on top of each other, there is a limit to the amount of ink that can be put on the substrate. This maximum total dot percentage is referred to as either Total Ink Coverage (TIC) or Total Area Coverage (TAC). When this technical limitation is ignored, the ink that gets laid down last wont attach properly to the previous layers leading to muddy browns in neutral areas. The ink also will not dry properly. This can cause set-off where the ink of a still wet substrate rubs off on whatever is stacked on top of it. Moreover, while manufacturers want to boost ink usage, customers would like to reduce ink consumption with minimum influence on color quality. Sometimes, these restrictions result in the loss of the color gamut. Anyway, the problem of ink feed control is crucial. To solve this problem, the manufacturers of RIP systems and printing equipment recommend to be guided

by different criteria such as: visual assessment by spreading or wicking, numerical evaluation of the color coordinates optical density, etc. However, so far any complete model that predicts the behaviour of ink in terms of its limited supply in inkjet printing has not been proposed.

In general, due to the printing process, the deposited ink surface coverage is larger than the nominal coverage resulting in a physical dot gain responsible for the ink spreading, which depends on the inks, on the substrate, and, also, on some other factors [1]. Spectral reflection prediction models are helpful in studying the impact of different factors influencing the range of printable colors (the inks, the substrate, the illumination conditions, and the halftones) and in creating printer characterization profiles for the purpose of color management [2]. The KubelkaMunk model (1) is widely used to predict the properties of multiple layers of ink overlaid at a given location, given information about each constituent inks reflectance and opacity [3],

$$\frac{K(\lambda)}{S(\lambda)} = \frac{(1 - R_\infty(\lambda))^2}{2R_\infty(\lambda)}, \tag{1}$$

where K is absorption and S is scattering coefficients, R_∞ is the reflectance of an infinitely thick sample and the prediction of S and K from reflectance is made at a given wavelength λ. Formula (1) allows predicting the combined K and S coefficients for multiple inks

$$K(\lambda) = K_B(\lambda) + \sum_{i=1}^{l} c_i K(\lambda), \tag{2}$$

where B refers to the substrate, l is the number of ink layers, c_i is the concentration and Ki is the absorption coefficient of the i-th layer. $S(\lambda)$ is computed similarly.

One of the first integrated color prediction models is the Neugebauer one, which predicts the CIEXYZ tristimulus values of a color halftone patch as the sum of the tristimulus values of their individual colorants [4]. Since the Neugebauer model neither takes explicitly into account the lateral propagation of light within the paper bulk nor the internal reflections at the paper-air border, its predictions noted as inaccurate. Most of up-to-date papers are connected with the YuleNielsen modified spectral Neugebauer (YNSN) model, which is the most well-known among the existing spectral reflection prediction models, where the YuleNielsen relationship applied to the spectral Neugebauer equations [5, 6]

$$R(\lambda) = (\sum_{i=1}^{p} w_i P_i(\lambda)^{\frac{1}{n}})^n, \tag{3}$$

where $R(\lambda)$ is the reflectance of a halftone pattern neighbourhood that is optically integrated as it is being viewed, w_i is the relative area coverage of the i-th Neugebauer Primary P, n is the Yule-Nielsen non-linearity that accounts for optical dot gain.

The further enhancement of the model (EYNSN) takes into account the ink spreading effect connected with the respective physical dot gains of one ink halftone printed in different superposition conditions (single ink and its combinations with 1–3 another colorants). The model uses multiple ink spreading curves (tone reproduction curves, TRC) to characterize the physical dot gain of the ink halftones on paper and in all solid ink superposition conditions [7]. With an ink-spreading model accounting for physical dot gain, a spectral reflection prediction models are able to predict reflectance spectra as a function of ink surface coverage for 3–4 inks [1, 8]. Minimization of difference metric between measured and predicted reflection spectrum for each superposition condition takes the effective ink surface coverage and the ink-spreading curve mapping nominal to effective surface coverage for each colorant.

Garg et al. [9] worked with calibrating the YNSN model with ink spreading curves derived from digitized RGB calibration patch images. They carried out spectral predictions with the ink spreading curves calibrated by relying on RGB images of 36 C, M, and Y patches (without black channel). For calculating the ink spreading curves, only 25%, 50%, and 75% nominal coverage are used in each superposition condition. In addition, for the broadband Yule–Nielsen equation [7, 10], they used the digitized RGB images of the paper white, the solid inks, and all the solid ink superposition. The model is tested on 729 patches comprising all nominal surface coverage combinations of 0%, 13%, 25%, 38%, 50%, 63%, 75%, 88%, and 100%. For comparison, authors present the prediction accuracies with the calibration of the ink spreading curves performed by spectral fits according to the YNSN model. As a reference, they consider also a single ink spreading function per ink obtained by computing the effective surface coverage of single ink halftones printed on paper. The prediction results demonstrate that the full ink-spreading model deduced from RGB images yields a better prediction accuracy than the classical single ink dot gain relying on spectral fits. The full ink-spreading model relying on digitized RGB images shows a slightly lower accuracy compared with the one calibrated with measured reflection spectra. Thus, authors reduced the effort of calibrating the YNSN model accounting for full ink spreading by computing the nominal to effective surface coverage curves from digitized RGB images instead of ones from measured reflection spectra. For calibration of the model by digitized RGB images, a user needs to measure only the reflection spectra of the solid colorant patches (for 3 inks: 8 patches) and digitize one sheet containing all calibration patches (for 3 inks: 44 patches). By using images instead of spectra, the prediction accuracy is not much affected. Tests were carried out with 729 color patches covering the complete gamut of the output device. In the case of C, M, and Y ink, the mean CIELAB ΔE_{94} difference between predicted and measured reflection spectra for calibration by spectral fits was 1.00. When calibrating with digitized RGB images, the mean prediction difference is CIELAB $\Delta E_{94} = 1.29$.

Livens [11] describes multi-density ink calibration in a framework that includes ink limitation and linearization and proposes a technique called the multiple linearization, which allows one to achieve a predefined color response with

respect to more than one quantity by exploiting the additional degrees of freedom offered by similarly colored inks. The method aimed to improve the visual uniformity. Since the transition between light and dark inks could result in some artefacts caused by too large amount of ink, the process of ink transition management must be under strict control. However, a key characteristic of existing ink mixing solutions is that they define the mapping in a fixed way independently of the calibration. The mapping is usually empirically optimized for a certain condition of the printer that might vary over time. The author proposes replacing the fixed ink mixing by a calibrated ink mixing that implies the multiple linearization, in which ink increments are computed conforming to equal increments or decrements in the measured variable. However, the measured value implies a set of different solutions, corresponding with various ratios of light and dark inks. The choice is done by constructing a calibration that results in more uniform CIELAB E steps. The linearization covers only that pair of CIELAB coordinates (L, a, b), which contributes much more to CIELAB ΔE. In fact, the major contribution is made by the chromatic coordinate (a, b). In geometrical interpretation, with single and multi-density inks, a 1D trajectory is described in the 3D color space by varying the ink percentage. The author suggests the linearization means dividing the trajectory into steps that correspond to an equal change in a measured variable. The author also agrees that it is often useful or even necessary to set ink limitations in order to cut off areas that cause problems in linearization. However, there is no description of curves behaviour and no suggestions how to manage ink limits.

In work [12], the objective was to quantify the influence of inkjet printer (Epson Pro 5000) calibration and profile–making on the quality of color reproduction in the context of fine art printing on a special paper compared with those obtained on a coated paper. The first step of the experiment was a fine setting of the printer in order to stabilize the results. The second step was a complete printer characterization with profile-making when different input parameters (total ink coverage, black ink limit, etc.) were adjusted. The performance of the color profiles was analyzed by color differences (CIELAB ΔE), the volume of color gamut, and spectral characteristics of the printed colors. Then the profiles were edited and optimized in order to reduce the color differences. The authors emphasize the importance of calibration (or linearization) because the tone increase value for inkjet printing is generally larger than for the other printing processes. They also agree that the determination of the limit TAC accepted by a paper is crucial in order to avoid problems such as poor ink drying and smudges. The typical value of TAC for inkjet on coated paper was indicated as 250%. Test-charts like IT8–7/3 are pointed to be a possible way for such a determination, as well as, for obtaining the grey balance. The ICC profiles are expected to be the overriding part of characterization. The authors conducted a conventional inkjet characterization where dot gains were calculated by Murray-Davis model. They received the predictable results where no significant difference was noticed between the two types of paper regarding the shape of the dots and dot–gain, which was just slightly lower in the case of the coated paper. During the TAC determination, the

amount of ink supply was assessed visually when for the limit of 280% there was a problem of ink migration towards the adjacent patches. Besides, there was a strong difference with the coated paper, which accepts higher the ink superimpositions. The best TAC (160%) was chosen by minimal CIELAB ΔE variation. As a result, the work did not demonstrate a substantial scientific novelty, however, showed the typical way, by which experts go when calibrate printing equipment. The problem of ink limitation occurs only in the process of building the profiles when the majority of the settings have been already committed.

Paper [13] is connected to ink consumption while achieve an accurate digital color reproduction by Epson Stylus Pro 4800 inkjet printer on different non-paper-substrates of POP display media. The assessments were done by measuring the raw linearization targets, which display color cast. The X-Rite i1–iO spectrophotometer was used as a measurement device. The ink usage was determined in terms of amount of ink restriction. A linearization test target was used to exam the inkjet hooking phenomena, i.e. the ink hue shifting associated with inkjet printers. It is noted that the color shift happens in chromatic and neutral shadow areas of a print due to impurities in the inkjet inks. For the DuPont Tyvek substrate, a typical inkjet hooking phenomena (for C and M channels) has been observed when printing with full ink load (see Fig. 1(a)).

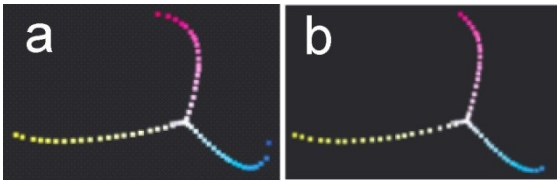

Fig. 1. Color hooking phenomena before (a) and after (b) ink reduction.

It shows the hue angle of cyan color begins to shift from a cyan blue to a contaminated cyan that turns purple because there is more red color in the cyan. The hue angle of magenta color shifts toward the yellow one. With further ink restriction (-16.25%), the inkjet hooking has been reduced, and ink distributed more evenly and correctly on the media (see Fig. 1(b)). At the same time, the ink restriction reduced the size of the color gamut: 16.25% ink reduction cut down the size of color gamut about 9%. A similar effect was observed for the Polypropylene, Satin Cloth, and Vinyl substrates. It was concluded that it is necessary to experiment with different linearization settings to achieve the right amount of ink distributed over the media. Each individual ink channel should be restricted just right after the color begins to change hook from the basic primary color while leaving extra color to extend the gamut for spot colors. Despite observation the phenomena, the authors did not revealed the cause and offered only empirical estimates of ink reduction.

Gradation scales are known as an indispensable attribute of color printing systems settings [14]. At the same time, the authors express doubts about the

rational use of these characteristics in digital (not analogue) printing technology. The problem, we believe, is that using the gradation curves in conventional 2D embodiment significantly reduces the quantity and quality of information extracted from them.

Thus, the work is devoted to building such a model, which is able to rectify the shortcomings of existing models.

2 Approach for the modelling

Let a gradation trajectory be the locus of points in the CIELAB space, which coordinates are consistent with the individual fields of measurement of the tone scale, arranged in ascending order of percentage of raster cells coverage in the layout of 0% (unsealed substrate) to 100% (die). Tone scales generally comprise no more than two dozen of fields, i.e., in practice, the gradation trajectory is represented by a discrete set of points in the CIELAB space. Contemporary printing systems provide a color depth of at least 256 gradations (8 bits), so the color change characteristics (hue, saturation, and brightness), as well as, the color coordinates might be assumed as a continuous function of the percentage (proportion) of raster cell filling. In other words, we can expect a nearly continuous change of color characteristics when filling percentage of a raster cell changes continuously.

If we took the percentage of raster cell filling as a parameter of a curve t, the gradation trajectory might be set by the parametric equations

$$\begin{cases} t \in [0;1], \\ L = c_{4L} \cdot t^4 + c_{3L} \cdot t^3 + c_{2L} \cdot t^2 + c_{1L} \cdot t + c_{0L}, \\ a = c_{4a} \cdot t^4 + c_{3a} \cdot t^3 + c_{2a} \cdot t^2 + c_{1a} \cdot t + c_{0a}, \\ b = c_{4b} \cdot t^4 + c_{3b} \cdot t^3 + c_{2b} \cdot t^2 + c_{1b} \cdot t + c_{0b}, \end{cases} \tag{4}$$

where $c_{ij} (i = \overline{0,1,2,3,4}, j = \overline{L,a,b})$ are some numerical coefficients. The interval of parameter t alteration is accepted from 0 (unsealed material) to 1 (100% die).

Since we have agreed to assume functions (1) to be continuous on the segment, then, according to the Weierstrass approximation theorem [15], their analytical form could be given by a polynomial of a certain extent. The theorem proves that if f is a continuous real-valued function on [a,b] and if any $\epsilon > 0$ is given, then there exists a polynomial p on $[a, b]$ such that $|f(x) - p(x)| < \epsilon$ for all x in $[a, b]$. In other words, any continuous function on a closed and bounded interval can be uniformly approximated on that interval by polynomials to any degree of accuracy. In our case, the polynomial of the fourth degree is required to detect such features of a space curve as the curvature (κ) and the torsion (τ) [16] because in the process of calculating the derivatives respect to a parameter up to the third power are used

$$r = (a(t), (t), c(t)), \kappa = \frac{|r' \times r''|}{|r'|^3}, \tau = \frac{(r' \times r'') \cdot r'''}{||r' \times r''||^2} \tag{5}$$

One should note that the ink spreading on solid surfaces and penetration into porous matrices (coated and uncoated papers) is described by power-law exponents [17].

3 Experiment

For the experiment, the 4-color (CMYK) wide-format solvent inkjet printer Mimaki CJV30-160BS was used. Print mode: 720 × 720 dpi, variable dot. Substrate: coated paper MediaPrint Gloss, 115 g/m^2 as a non-absorbent paper and the drawing paper, 200 g/m2 as a highly absorbent material. The measurement tools: spectrophotometer x-Rite iOne iSis + x-Rite ProfileMaker package.

Tone scales containing 50 bitmap fields were synthesized using the ChartGenerator – MeasureTool in ProfileMaker design for the automatic iOne iSis. Sample scales were printed by swastika on the same sheet in order to average the results of scale measurement depending on the print direction and printing head motion in relation to the layout. At one act of the experiment, two sheets were printed. The results of the 8 measurements were averaged in ProfileMaker–MeasureTool and saved as a text file, which then was imported into the MS Excel. There it stood out as a matrix of variables of dimension 51 (50 raster fields plus the unsealed material) × 4 (the proportion of a raster cell filling plus CIELAB coordinates values). The measured data were divided into individual color channels. Matrix variables, which contained t, L, a, b data of each color patch as columns, were imported into the MatLab where they were used in further mathematical processing.

The approximation of dependences (5) by polynomials was implemented in the MatLab package using the fit function. It is necessary to ensure a minimum cumulative CIELAB ΔE_{76} [18] color difference between the theoretical trajectory and experimental points. In controversial cases, a preference was given to a lesser degree polynomial. The value of the total color difference CIELAB ΔE_{76} of experimental points from the theoretical trajectory was 4–7 units. For comparison, the worst deviation from the average in the preparation of the experimental points was 1.5–2 color difference CIELAB ΔE_{76} units.

4 Results and discussion

As for any other continuous space curve, the numerical factors such as the curvature and torsion in terms of differential geometry can be defined at each point of the gradation trajectory. Figure 2 shows a gradation trajectory for the Magenta color channel. The points correspond to the tone scale fields variation, the solid curve is a gradation trajectory, at the bottom there is the projection of the trajectory onto the *ab* chromaticity plane. Figure 3 shows the dependencies of curvature and torsion on the degree of filling of the raster element. As it is seen, the curvature of the trajectory is different from zero in almost all shades of the range. This means that the path is not straight. The presence of local extrema points to a jerky change of hue while a raster cell is being filled.

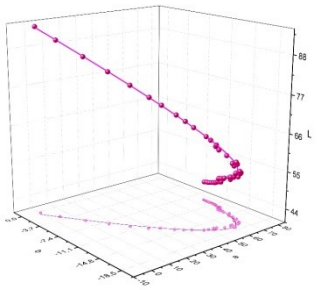

Fig. 2. Gradation trajectory for the *Magenta* channel.

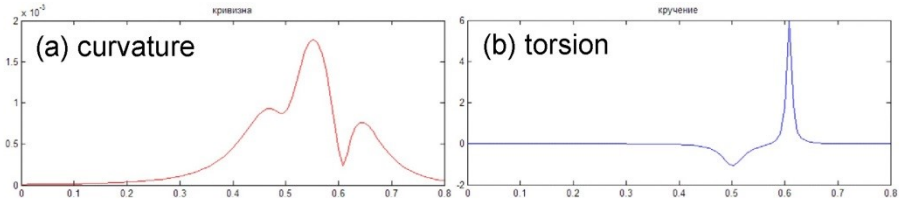

Fig. 3. Curvature (a) and torsion (b) values for the gradation trajectory depending on the proportion of filling of the raster element.

The presence of fields that are significantly different from zero in the torsion chart says that the gradation trajectory is not a flat curve that can be regarded as the main reason for the problems encountered in the inkjet printers linearization.

5 Conclusions

A new three-dimensional interpretation of the gradation curves in Lab-space is proposed. Gradation trajectories, as well as, the method of their analytical description are described. Gradational trajectories are conceived as continuous and bounded on the gradation range curves. In this connection, the apparatus of differential geometry of curves is applied to them and the values of such parameters as curvature and torsion were calculated.

Unfortunately, there is still no sustainability criterion, which can be used for certain specification of maximum percentage of the ink supply. Possible options for such a criterion, for example, can be a first maximum in the plot of curvature or the point, at which the torsion becomes significantly different from zero.

Search of this criterion is the direction of the future investigations.

Gradation trajectories introduced in the described manner are the global features of inkjet printing process that are depended on type of the paper and properties of the ink only. Note that they are not affected by rasterizing method, number of passes, and measuring technique.

Any limitation of ink supply and any method of linearization under the conditions of a tone scales print will give the family of the points belonging to

the gradation trajectory. In other words, if the printing conditions mentioned are met, then regardless of the selected ink supply limitations the results of measurement of gradation scales will form a family of points on the gradation trajectories describing each color channel.

References

1. Balasubramanian R. Optimization of the spectral Neugebauer model for printer characterization. Journal of Electronic Imaging, 8, 156166. (1999)
2. Bala R. Device characterization. Digital Color Imaging Handbook, ed. G. Sharma (CRC Press, Boca Raton, FL), 269379 (2003)
3. Kubelka P. & Munk F. Ein Beitrag zur Optik der Farbanstriche, Zeitschrift fur technische Physik, Germany, 12, 593601 (1931)
4. Neugebauer H.E.J. Die theoretischen Grundlagen des Mehrfarbendrucks. Zeinschrift fur Wissenschaftliche Photographie Photophysik Photochemie, 36, 3673 (1937)
5. Yule J. A. C. & Nielsen W. J. The penetration of light into paper and its effect on halftone reproductions. Proc. TAGA Conference 1951 (TAGA, Sewickley, PA), 6576 (1951)
6. Viggiano J. A. S Modeling the color of multi-colored halftones. Proc. TAGA Conference 1990 (TAGA, Sewickley, PA), 4462 (1990)
7. Hersch R.D. & Crete F. Improving the YuleNielsen modified spectral Neugebauer model by dot surface coverages depending on the ink superposition conditions. Proc. SPIE 5667, 434445 (2005)
8. Wyble D.R. & Berns R.S. A critical review of spectral models applied to binary color printing. Color Research & Application, 25, 419 (2000)
9. Garg N.P., Singla A.K. & Hersch R.D. Calibrating the YuleNielsen Modified Spectral Neugebauer Model with Ink Spreading Curves Derived from Digitized RGB Calibration Patch Images. Journal of Imaging Science and Technology 52(4), 040908040908-5 (2008)
10. Arney J.S., Engeldrum P.G., & Zeng H. An expanded Murray-Davis model of tone reproduction in halftone imaging. Journal of Imaging Science and Technology, 39, 502508 (1995)
11. Livens S. Optimisation of Printer Calibration in the Case of Multi Density Inks. Conference on Color in Graphics, Imaging, and Vision, CGIV 2002 Final Program and Proceedings, 633638 (2002)
12. Chagas L., Blayo A. & Giraud P. Color Profile: methodology and influence on the performance of ink-jet color reproduction. IS&T's NIP20: 2004 International Conference on Digital Printing Technologies, 655659 (2004)
13. Wu Y-J. Reducing Inkjet Ink Consumption with RIP software for POP Display Media. Digital Fabrication and Digital Printing: NIP30 Technical Program and Proceedings, 108111 (2014)
14. Kipphan H. Handbook of Print Media. Springer-Verlag Berlin Heidelberg, 1207p (2001)
15. Jeffreys H. & Jeffreys B. S. Weierstrass's Theorem on Approximation by Polynomials and Extension of Weierstrass's Approximation Theory. §14.08-14.081 in Methods of Mathematical Physics, 3rd ed. Cambridge, England: Cambridge University Press, 446448 (1988)
16. Pogorelov A.V. Differential geometry. Noordhoff, 171p (1959) (Translated from Russian)

17. Rosenholm J.B. Liquid spreading on solid surfaces and penetration into porous matrices: Coated and uncoated papers. Advances in Colloid and Interface Science, Vol. 220, 853 (2015)
18. Pauli H. Proposed extension of the CIE recommendation on "Uniform color spaces, color difference equations, and metric color terms". Journal of the Optical Society of America, Vol. 66, 866867 (1976)